Photosynthetic Antenna−Reaction Center Mimicry: Sequential Energy- and Electron Transfer in a Self-assembled Supramolecular Triad Composed of Boron Dipyrrin, Zinc Porphyrin and Fullerene

Eranda Maligaspe,[†] Nikolai V. Tkachenko,*[,‡] Navaneetha K. Subbaiyan,[†] Raghu Chitta,[†] Melvin E. Zandler,[†] Helge Lemmetyinen,[‡] and Francis D'Souza*[,†]

Department of Chemistry, Wichita State University, 1845 Fairmount, Wichita, Kansas 67260-0051, and Tampere University of Technology, P.O. Box 541, 33101 Tampere, Finland

Received: April 7, 2009; Revised Manuscript Received: June 8, 2009

A self-assembled supramolecular triad, a model to mimic the photochemical events of photosynthetic antenna−reaction center, viz., sequential energy and electron transfer, has been newly constructed and studied. Boron dipyrrin, zinc porphyrin, and fullerene respectively constitute the energy donor, electron donor, and electron acceptor segments of the antenna−reaction center mimicry. For the construction, first, boron dipyrrin was covalently attached to a zinc porphyrin entity bearing a benzo-18-crown-6 host segment at the opposite end of the porphyrin ring. Next, an alkyl ammonium functionalized fullerene was used to self-assemble the crown ether entity via ion−dipole interactions. The newly formed supramolecular triad was fully characterized by spectroscopic, computational, and electrochemical methods. Selective excitation of the boron dipyrrin moiety in the dyad resulted in energy transfer over 97% efficiency creating singlet excited zinc porphyrin. The rate of energy transfer from the decay measurements of time-correlated singlet photon counting (TCSPC) and up-conversion techniques agreed well with that obtained by the pump−probe technique and revealed efficient photoinduced energy transfer in the dyad (time constant in the order of 10−60 ps depending upon the conformer). Upon forming the supramolecular triad by self-assembling fullerene, the excited zinc porphyrin resulted in electron transfer to the coordinated fullerene yielding a charge-separated state, thus mimicking the antenna−reaction center functionalities of photosynthesis. Nanosecond transient absorption studies yielded a lifetime of the charge-separated state to be 23 μs indicating charge stabilization in the supramolecular triad. The present supramolecular system represents a successful model to mimic the rather complex "combined antenna−reaction center" events of photosynthesis.

Introduction

The photochemical process of natural photosynthesis involves two major steps, namely, absorption and transportation of light energy of appropriate wavelength by the antenna light harvesting molecules to the reaction center and occurrence of photoinduced electron transfer (PET) to generate charge-separated entities by using the electronic excitation energy.[1] The light energy harvesting antenna system consists of chromophore arrays which transport energy via a singlet−singlet energy transfer mechanism among the chromophores. The antenna pigments, different for different organisms, are optimized for the quality of light in a particular environment and are effectively coupled to the reaction center. The reaction center absorbs the excitation energy and converts it to chemical energy in the form of transmembrane charge separation via a multistep electron transfer reaction. The stored electrochemical energy in the form of charge-separated species is later converted into other forms, e.g., proton motive force, of biological useful forms of energy.[1]

Mimicry of the photosynthetic events by using synthetic model compounds is vital to further our understanding of the complex processes of bioenergetics. Research in this area also holds promise for technological advances in light energy harvesting, building molecular optoelectronics, and to develop photocatalysts capable of producing hydrogen.[2] In this regard, several studies using synthetic models focused on mimicking the reaction center where photoinduced electron transfer from the excited donor to acceptor occurs have been reported.[3−11] In the majority of these studies porphyrin has been used as an electron donor due to its close resemblance to the photosynthetic pigment, chlorophyll, and the established synthetic manipulations. The efficiency of charge separation in some of the donor−acceptor systems has been comparable to those found in natural reaction centers.[7d,e] To mimic the antenna functionality, singlet−singlet energy transfer between two or more covalently linked or self-assembled porphyrins, or other chromophores, has been studied extensively.[12−16] Some of these molecular/supramolecular systems have revealed potentials for constructing photonic, photocatalytic, and optoelectronic devices.[2,17,18]

Although a number of studies dealing either with the reaction center or the antenna mimicry have been reported,[3−16] a molecular/supramolecular complex performing combined antenna and reaction center functions has been scarce. A very few elegantly designed molecular/supramolecular systems involving two or more fluorophores and an electron acceptor like fullerene have been developed and the occurrence of stepwise energy and electron transfer events has been demonstrated.[19−21] In the present study, we report a self-assembled supramolecular complex to perform the combined antenna−reaction center photochemical events. The structure of the model system is

* To whom correspondence should be addressed. E-mail: francis.dsouza@wichita.edu and nikolai.tkachenko@tut.fi.
[†] Wichita State University.
[‡] Tampere University of Technology.

10.1021/jp9032194 CCC: $40.75
Published on Web 07/06/2009

SCHEME 1: Structure of the Presently Constructed Supramolecular Triad Composed of Boron Dipyrrin−Zinc Porphyrin−Crown Ether Bound to an Alkyl Ammonium Functionalized Fulleropyrrolidine to Probe "Antenna−Reaction Center" Functionalities[a]

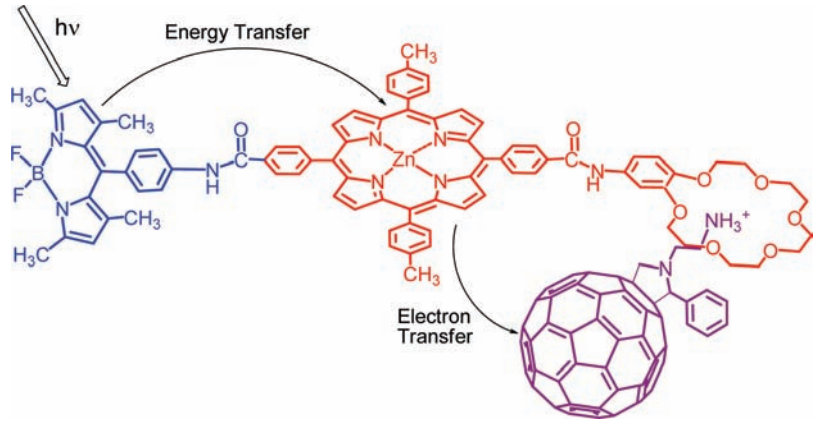

[a] The photochemical events occurring in the triad are shown by the arrows.

shown in Scheme 1. Here, boron dipyrrin[22a] (also known as BODIY, abbreviated as BDP) acts as an energy absorbing and transferring antenna to the light energy acceptor, zinc porphyrin. That is, when excited in the 480−515 nm wavelength region, selective excitation of BDP occurs,[21a,22] and due to good spectral overlap between BDP emission and zinc porphyrin absorption spectra, efficient singlet−singlet energy transfer to the zinc porphyrin takes place. When the crown ether receptor site of the dyad binds to an electron acceptor, an alkyl ammonium bearing fulleropyrrolidine,[23] photoinduced electron transfer from the singlet excited porphyrin to fulleropyrrolidine subsequently occurs. The present model compound differs from the earlier reported one by us[21a] in which instead of metal−ligand axial coordination, a crown ether−crown binding approach has been employed. The easily oxidizable BDP unit in the present system is also involved to some extent in stabilizing the charge-separated state. The stronger crown ether−crown binding approach permits us to perform the investigations in an electron transfer favoring solvent such as polar benzonitrile.[23] Systematic spectral, computational, electrochemical, and photochemical studies have been performed to unravel sequential energy and electron transfer in the newly built supramolecular triad.

Results and Discussion

Syntheses. The synthesis of BDP−ZnP−crown ether involved a multistep procedure as outlined in Scheme 2. First, 5-(4-methoxycarbonylphenyl)dipyrromethane was prepared by the reaction of pyrrole and methyl 4-formyl benzoate according to the Lindsey procedure.[24] The dipyrromethane was subsequently reacted with *p*-tolylaldehyde followed by chloranil oxidation to obtain 5,15-di(methoxycarbonylphenyl)-10,20-di-(tolyl)porphyrin.[25] The ester groups were subsequently hydrolyzed in THF:ethanol, using KOH to obtain H_2-5,15-di(*p*-carboxyphenyl)-10,20-di(*p*-tolyl)porphyrin.

The BDP derivative, 1-(difluoroboryl)-2-[(*Z*)-(3,5-dimethyl-2*H*-pyrrol-2-ylidene)(4-nitrophenyl)methyl]-3,5-dimethyl-1*H*-pyrrole, was prepared by the reaction of 2,4-dimethylpyrrole and nitrobenzaldehyde in the presence of trifluoroacetic acid in CH_2Cl_2.[19d] The nitro group was subsequently reduced to the amino group by the hydrogenation reaction, using Pd on charcoal catalyst followed by purification by flash chromatography on a silica gel column.

Finally, the BDP−porphyrin−crown ether, H_2-5-{4-[2-(4-benzo-[18-crown-6])amido]phenyl}-15-{4-[2-(4-difluoroboron dipyrrinylphenyl)amido]phenyl}-10,20-di(*p*-tolyl)porphyrin, was prepared by reacting equimolar amounts of the acid chloride form of 5,15-di(methoxycarbonylphenyl)-10,20-di(tolyl)-porphyrin, 1-(difluoroboryl)-2-[(*Z*)-(3,5-dimethyl-2*H*-pyrrol-2-ylidene)(4-aminophenyl)methyl]-3,5-dimethyl-1*H*-pyrrole, with 4′-aminobenzo-[18-crown-6] in dry toluene. Chromatographic separation followed by metalation with zinc acetate gave the desired product, 5-{4-[2-(4-benzo-[18-crown-6])amido]phenyl}-15-{4-[2-(4-difluoroboron dipyrrinylphenyl)amido]phenyl}-10,20-di(*p*-tolyl)porphyrinato zinc(II). The newly synthesized compound was stored in the dark prior to performing the experiments.

Ground State Properties of the Boron Dipyrrin−Zinc Porphyrin Dyad. Figure 1a shows the optical absorption spectrum of the dyad along with the spectra of control compounds in benzonitrile. 1-(Difluoroboryl)-2-[(*Z*)-(3,5-dimethyl-2*H*-pyrrol-2-ylidene)(4-tolyl)methyl]-3,5-dimethyl-1*H*-pyrrole as BDP control and 5-{[4-(benzo-[18-crown-6])amido]phenyl}-10,15,20-tri(*p*-tolyl)porphyrinatozinc(II) as zinc porphyrin−crown ether control were used. The absorption bands located at 431, 559, and 602 nm correspond to zinc porphyrin while the band at 495 nm corresponds to the boron dipyrrin entity (plot i in Figure 1a). The absorption band corresponding to BDP revealed ∼2 nm red shift in the dyad, indicating some ground state interactions between the two chromophores. Importantly, the absorption of boron dipyrrin at 504 nm had no appreciable overlap with the ZnP−crown ether control or C_{60} ammonium cation absorption at these wavelengths (plots ii and iv in Figure 1b). Hence, irradiation of the dyad at the 500 nm region is expected to a large extent to selectively excite the boron dipyrrin moiety of the dyad.[21a,22b]

The fluorescence emission spectrum of the BDP−zinc porphyrin dyad, excited at 495 nm corresponding to BDP excitation, is shown in Figure 1b along with the emission of control compounds. An emission band at 515 nm corresponding to the emission of BDP was observed in addition to the zinc porphyrin emission bands at 614 and 662 nm (Figure 1b, plot i). The area under the 515 nm band was found to be quenched over 93% compared to BDP control (plot ii in Figure 1b). In a control experiment, the emission spectrum of BDP control in the presence of an equimolar amount of zinc porphyrin−crown ether control was recorded. Under these conditions, the presence of zinc porphyrin had no effect on the BDP emission intensity; in addition, no significant emission corresponding to zinc porphyrin

SCHEME 2: Synthetic Procedure Adopted To Form the BDP−Zinc Porphyrin−Crown Ether Host System in the Present Study

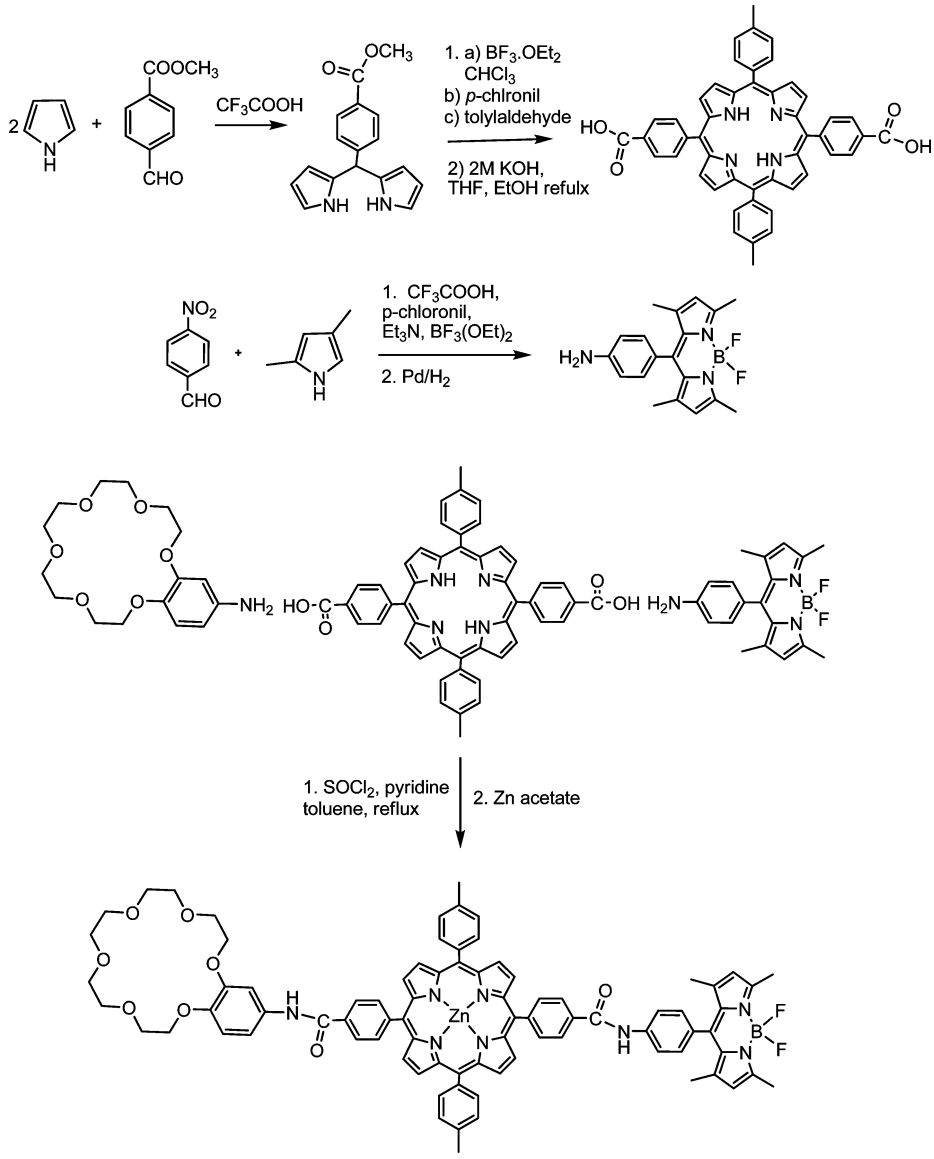

was observed. In separate control experiments, when ZnP−crown ether control and C_{60} ammonium cation were excited at 514 nm, no significant emission at 614 and 662 nm corresponding to ZnP in the former case or at 720 nm corresponding to fulleropyrrolidine in the latter case were observed (Figure 1b, plots iii and iv). These results suggest the absence of simultaneous excitation of the different chromophores used to build the triad in Scheme 1 when excited at 514 nm corresponding to BDP excitation, an important criteria to visualize sequential energy and electron transfer in "antenna−reaction center" mimics.

The occurrence of singlet excited energy transfer from BDP to zinc porphyrin in the dyad was also confirmed by recording the excitation spectrum of the dyad while holding the emission monochromator at 662 nm corresponding to zinc porphyrin emission. Such a spectrum shown in Figure 2 revealed the excitation band of not only the zinc porphyrin entity but also that of the BDP entity of the dyad indicating energy transfer from BDP to zinc porphyrin. An estimation of energy transfer was performed by calculating the intensity ratio of the BDP band at 504 nm to the zinc porphyrin visible band at 559 nm (S_o to S_1 transition) in the absorption spectrum of the dyad in Figure 1a, and in the excitation spectrum of the dyad in Figure 2. The peak intensity ratio from the absorption spectrum was found to be 4.1 while for the excitation spectrum this ratio was 4.05 amounting to an energy transfer efficiency of about 97%. These observations suggest excited energy transfer as the exclusive quenching mechanism in the BDP−zinc porphyrin dyad.

Formation of the Supramolecular BDP−ZnP−Fullerene Triad

The formation of the supramolecular triad was initially followed by optical absorption and steady-state fluorescence methods. Figure 3 shows the spectral changes observed during the addition of C_{60} alkyl ammonium cation to the BDP−ZnP crown ether dyad in benzonitrile. The absorption bands corresponding to both the zinc porphyrin and BDP entities revealed a slight increase in their intensity without any noticeable changes in the peak position. The increase in absorption in the 350 nm region is due to the presence of fulleropyrrolidine in solution. Extending the absorption wavelength well into the near-IR region revealed no new bands corresponding to any charge

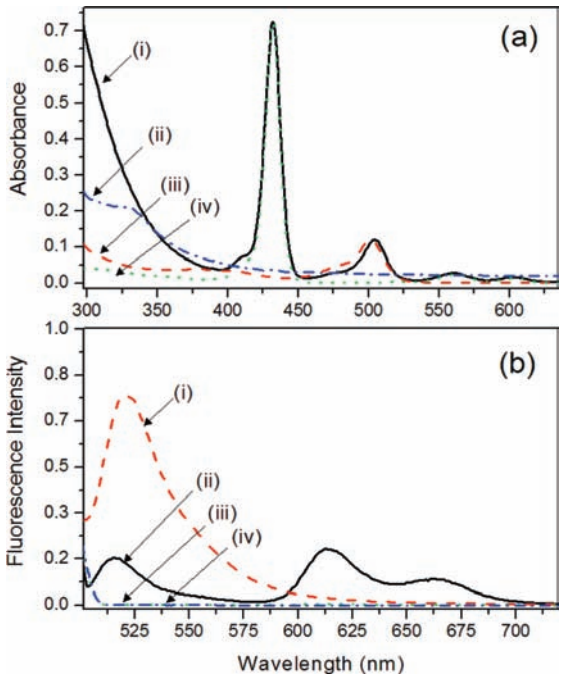

Figure 1. (a) UV−visible spectra of (i) BDP−zinc porphyrin−crown ether dyad (0.32 μM), (ii) C_{60} ammonium cation (0.12 mM), (iii) *p*-tolyl boron dipyrrin (BDP control, 0.32 μM), and (iv) zinc porphyrin−crown ether (0.32 μM) in benzonitrile. (b) Fluorescence spectra of (i) BDP control (0.32 mM), (ii) BDP−zinc porphyrin−crown ether dyad (0.32 μM), (iii) zinc porphyrin−crown ether control (0.32 μM), and (iv) C_{60} ammonium cation (0.12 mM) in benzonitrile. The compounds were excited at λ_{ex} = 495 nm.

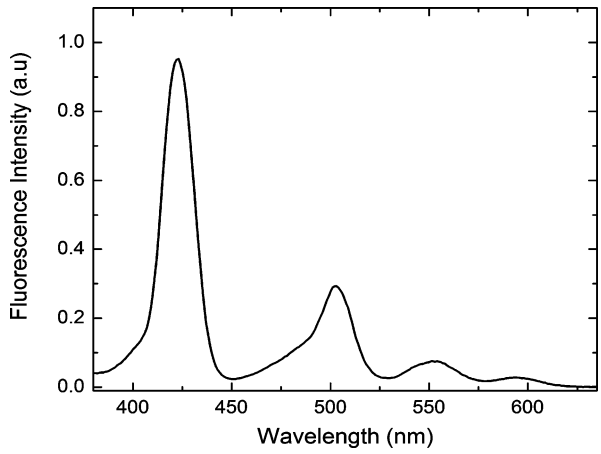

Figure 2. Excitation spectrum collected at 662 nm of the boron dipyrrin−zinc porphyrin dyad in benzonitrile.

transfer complex. These observations suggest little, if any, interactions between the fullerene and either the zinc porphyrin or BDP entities. That is, a nonperturbed electronic structure of the zinc porphyrin and BDP chromophores upon formation of the triad via crown ether−alkyl ammonium binding is borne out from this study.

The fluorescence spectrum recorded during the formation of the supramolecular triad revealed drastic quenching effects. As shown in Figure 4a, increasing addition of fulleropyrrolidine to the BDP−zinc porphyrin dyad solution quenched the fluorescence of not only the zinc porphyrin but also that of BDP suggesting the occurrence of excited state events. In a control experiment, the emission of BDP−zinc porphyrin dyad was monitored by increasing the addition of 2-phenylfulleropyrrlidine, that is, fulleropyrrolidine bearing no alkyl ammonium

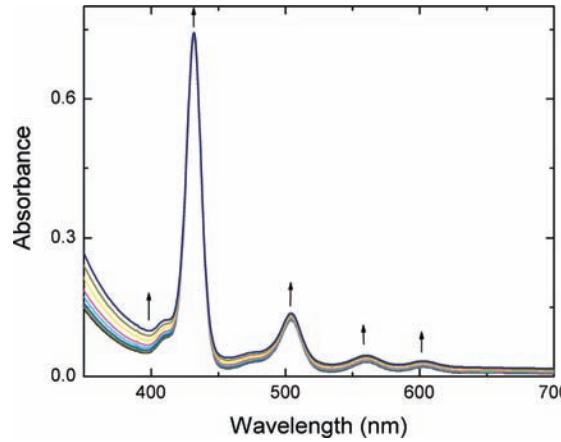

Figure 3. Absorption spectral changes observed during titration of BDP−zinc porphyrin−crown ether (3.6×10^{-6} M) binding to C_{60} ammonium cation (2.4×10^{-4} M each addition) in benzonitrile.

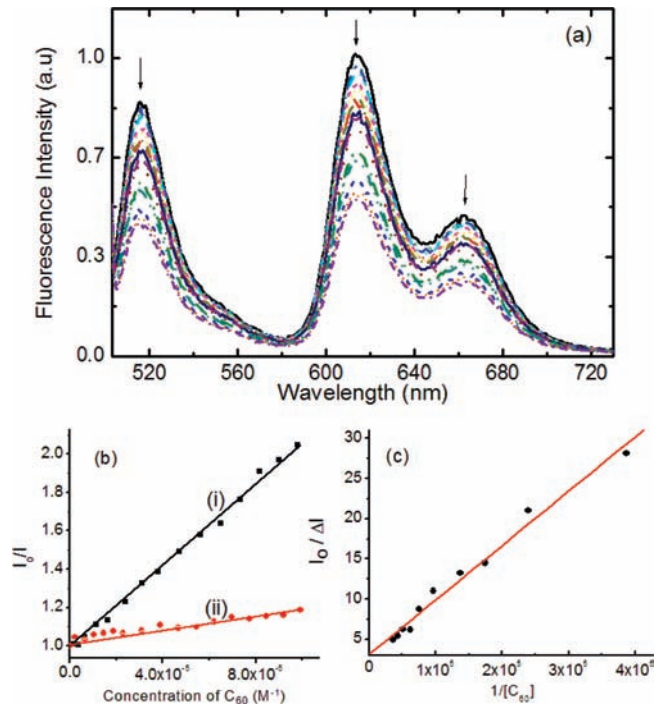

Figure 4. (a) Fluorescence spectral changes observed during increasing addition of C_{60} ammonium cation (0.24 mM each addition) to a solution of BDP−zinc porphyrin−crown ether to form the triad in benzonitrile. λ_{ex} = 495 nm. (b) Stern−Volmer plots constructed for (i) C_{60} ammonium cation and (ii) 2-phenyl fulleropyrrolidine quenching of BDP−zinc porphyrin−crown ether in benzonitrile (emission intensity of the 614 nm band of zinc porphyrin was monitored). (c) Benesi−Hildebrand plot constructed by monitoring the emission intensity at 614 nm band for calculating the binding constant. The abbreviations I_o and I represent fluorescence intensity in the absence and presence of fullerene, and ΔI is the change of fluorescence intensity upon addition of fullerene.

functionality. Stern−Volmer plots of zinc porphyrin quenching monitored at 614 nm were constructed as shown in Figure 4b; a higher slope was obtained for C_{60} alkyl ammonium cation binding to the dyad. The calculated Stern−Volmer constant, K_{SV}, was found to be 1.06×10^5 M^{-1} for C_{60} alkyl ammonium cation binding to the dyad, which compared with a value of 1.9×10^3 M^{-1} for 2-phenylfulleropyrrolidine binding to the dyad. The higher K_{SV} value for the former case unanimously proves C_{60} alkyl ammonium binding to the crown ether induced intramolecular quenching. The magnitude of K_{SV} for 2-phenyl-

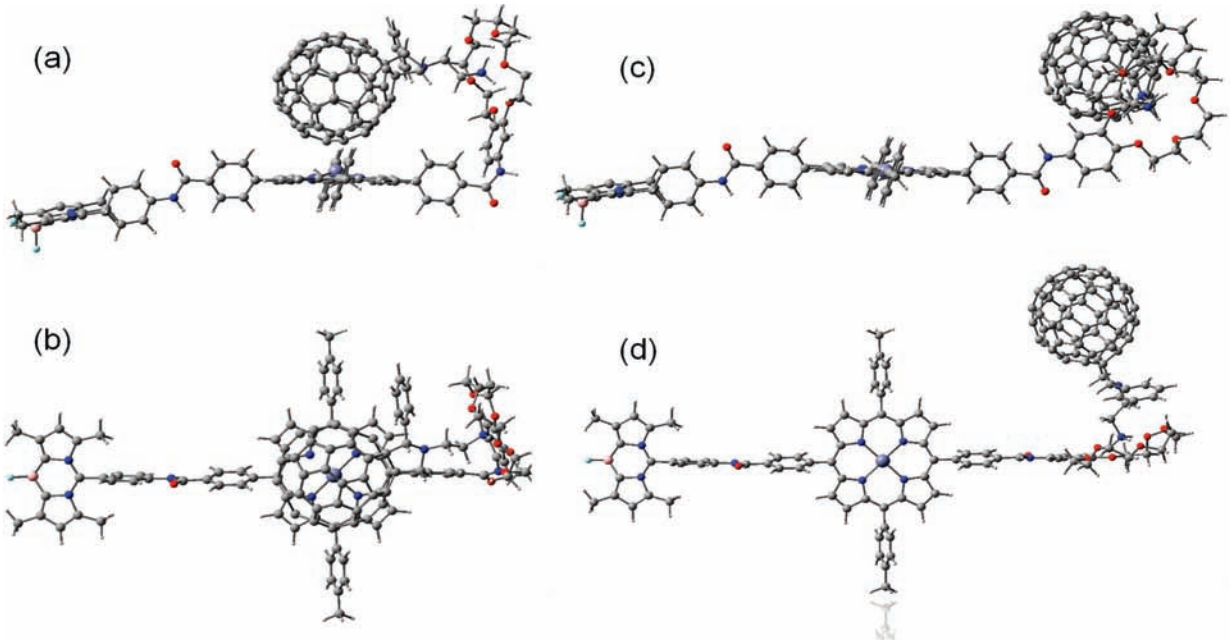

Figure 5. B3LYP/3-21G(*) optimized structures of supramolecular triad comprised of boron dipyrrin−zinc porphyrin−crown ether bound to C_{60} alkyl ammonium cation in the close (a and b) and extended (c and d) forms.

fulleropyrrolidine quenching is slightly larger than that predicted for a biomolecular quenching process.[26] This could be rationalized by the weaker porphyrin−fullerene and fullerene−crown ether interactions reported earlier.[27] To calculate the binding constant of crown ether−alkyl ammonium cation binding, the quenching data were analyzed by using the Benesi−Hildebrand method.[28] Such analysis yielded a straight line plot indicating a 1:1 complex formation (Figure 4c) and a binding constant, K, of 4.6×10^4 M^{-1}. The magnitude of the binding constant is comparable to the K values reported earlier for other crown ether−alkyl ammonium binding[23] suggesting stable complex formation in the studied benzonitrile solvent.

Geometry Optimization by Computational Calculations. The structure of the supramolecular triad was visualized by performing computational studies at the B3LYP/3-21G(*) level.[29,30] Figure 5 shows the optimized structures in two orientations of the triad in which two forms, viz., "close" and "extended", were visualized. Both of the structures were energetically stable as they revealed minima on a Born−Oppenheimer potential energy surface. The "close" form was energetically favored by ~7.6 kcal/mol, which could be attributed to the spontaneous attraction between porphyrin and fullerene[31] and the flexible nature of the benzo-18-crown-6 entity. However, this energy could be an overestimation due to a large Basis Set Superposition Errors (BSSE) as a result of the low-level B3LYP/3-21G(*) basis set.[38]

In the "close" form of the triad, the distance between the boron atom of BDP and the zinc of ZnP was 18.77 Å while the distance between the zinc and the center of C_{60} was found to be 5.59 Å suggesting closely disposed donor−acceptor entities. Similarly, the distance between boron and the center of C_{60} was found to be 20.47 Å being sufficiently far from the electron acceptor fullerene. In the "extended" form, the distance between the boron atom of BDP and the zinc of ZnP was 18.68 Å while the distance between the zinc and the center of C_{60} was found to be 18.59 Å suggesting distantly disposed donor−acceptor entities. The distance between boron and the center of C_{60} was found to be 35.03 Å being far from the electron acceptor fullerene. It is interesting to note that the boron dipyrrin and porphyrin macrocycles were in the same plane for both forms of the structures, which may facilitate energy transfer due to favorable macrocycle orientation.[26]

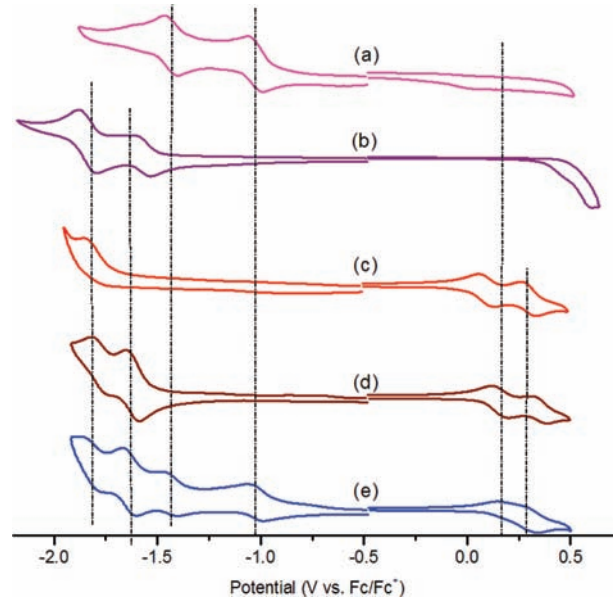

Figure 6. Cyclic voltammograms of (a) C_{60} alkyl ammonium cation, (b) *p*-tolyl boron dipyrrin (BDP control) (c) zinc porphyrin−crown ether, (d) BDP−zinc porphyrin−crown ether dyad, and (e) BDP−zinc porphyrin−crown ether−fullerene triad in benzonitrile containing 0.1 $(TBA)ClO_4$. Scan rate = 0.1 V/s.

Cyclic Voltammetry Studies and Estimation of Energy Levels. Electrochemical studies using the cyclic voltammetric technique were performed to arrive at the redox potentials of the newly assembled supramolecular triad. Figure 6 shows cyclic voltammograms of the investigated compounds along with the control compounds during both negative and positive scanning of the potential. The first two reductions of the C_{60} alkyl ammonium cation were located at $E_{1/2} = -1.03$ and -1.45 V vs. Fc/Fc^+, respectively (Figure 6a).[23a] The peak-to-peak separation and plots of peak current versus square root of scan rate

indicated both electroreductions to be one-electron reversible processes.[32] The one-electron reductions of the BDP control were located at $E_{1/2} = -1.56$ and -1.83 V vs. Fc/Fc$^+$ while its irreversible oxidations were located at $E_{pa} = 0.46$ and 0.61 V vs. Fc/Fc$^+$ (Figure 6b), respectively. The first two reversible oxidations of the zinc porphyrin−crown ether were located at $E_{1/2} = 0.11$ and 0.29 V vs. Fc/Fc$^+$ while the first irreversible reduction was located at $E_{pc} = -1.85$ V vs. Fc/Fc$^+$, respectively (Figure 6c). As shown in Figure 6d, the first two reversible oxidations of the BDP−zinc porphyrin crown ether dyad were located at $E_{1/2} = 0.17$ and 0.36 V vs. Fc/Fc$^+$ while the first two reversible reductions were located at $E_{1/2} = -1.61$ and -1.71 V vs. Fc/Fc$^+$, respectively. Control experiments involving pristine BDP and zinc porphyrin indicated that both these oxidations involve porphyrin macrocycle and not the BDP entity. By comparison of the redox potentials of starting control compounds in Figure 6a−c, the first reduction of the BDP−ZnP−crown ether dyad at -1.61 V was ascribed to the reduction of the BDP entity while the first oxidation at 0.17 was ascribed to the zinc porphyrin entity, respectively.

Addition of the C_{60} alkyl ammonium cation to the BDP−ZnP−crown ether dyad solution to form the supramolecular triad revealed noticeable changes in the redox potentials. That is, the first oxidation process of the zinc porphyrin revealed a slight positive shift and the second oxidation a slight negative shift, located at $E_{1/2} = 0.20$ and 0.28 V vs. Fc/Fc$^+$, respectively (Figure 6e). The small anodic shift of zinc porphyrin upon the formation of the triad suggests intramolecular interactions between the fullerene and zinc porphyrin entities, a result that readily agrees with the predictions of the earlier discussed computational results. As discussed earlier, our attempts to locate a new absorption band corresponding to charge transfer interactions in the near-IR region were not successful. Perhaps the extinction coefficient for such absorption band is too small to be detected even at relatively higher concentrations. The first two reductions of the supramolecular triad were located at $E_{1/2} = -1.00$ and -1.44 V vs. Fc/Fc$^+$, and by comparison with the redox potentials of the control compounds both processes were assigned to the one-electron reduction of the C_{60} alkyl ammonium cation. These values are close to that reported for similar fulleropyrrolidine derivatives in benzonitrile.[23] The third reduction process of the triad located at -1.62 V corresponding to BDP reduction revealed no significant changes as compared to the corresponding reductions of the dyad.

By using the electrochemical data, excited energies and distances between the chromophores, the free energies of charge separation (ΔG_{CS}), and charge recombination (ΔG_{CR}) were calculated, using eqs 1 and 2, by Weller's approach.[33]

$$\Delta G_{CR} = e(E_{ox} - E_{red}) + \Delta G_S \quad (1)$$

where $\Delta G_S = -e^2/(4\pi\varepsilon_0\varepsilon_R R_{Ct\text{-}Ct})$ and ε_0 and ε_R refer to vacuum permittivity and dielectric constant of benzonitrile.

$$-G_{CS} = \Delta E_{0-0} - \Delta G_{CR} \quad (2)$$

where ΔE_{0-0} is the energy of the lowest excited state of ZnP (2.05 eV).

Such calculations revealed a ΔG_{CS} value of -0.82 eV for electron transfer from the singlet excited zinc porphyrin to fullerene, and a ΔG_{CR} value of -1.18 eV for the charge recombination process, for both "close" and "extended" forms of the structures. For comparison purposes, the ΔG_{CS} and ΔG_{CR} values for charge separation within the BDP−zinc porphyrin, donor−acceptor dyad were also calculated. The ΔG_{CS} and ΔG_{CR} originating from the ^{1}ZnP*−BDP were found to be -0.41 and -1.63 eV, respectively. These studies, in addition to the thermodynamic feasibility of the occurrence of electron transfer, also indicate fullerene being the superior electron acceptor in the supramolecular triad.

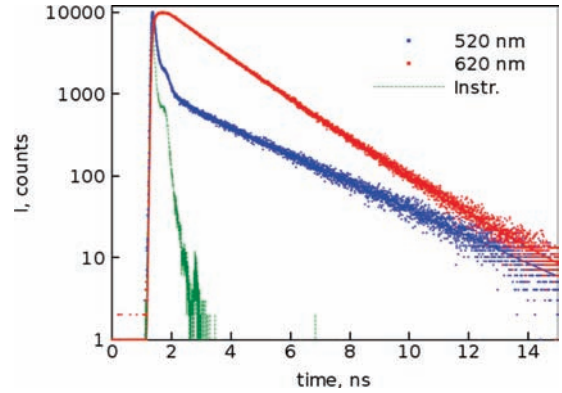

Figure 7. Emission decays of BDP−ZnP dyad in benzonitrile at 620 and 520 nm. The excitation wavelength was 485 nm. These measurements were carried out by using the TCSPC technique. The dashed line is the instrument response function.

Time-Resolved Emission and Transient Absorption Studies

The photodynamics of the energy and charge transfer of the newly developed dyad and triad was studied by pico- and femtosecond optical spectroscopy techniques. The emission decays measured by using the time-correlated single photon counting (TCSPC) method are shown in Figure 7. The boron dipyrrin−zinc porphyrin dyad in benzonitrile was excited at 485 nm. At this wavelength boron dipyrrin was mainly excited. The emission decays were monitored at 520 and 620 nm corresponding to the emission wavelengths of boron dipyrrin and zinc porphyrin fluorescence, respectively. The data could be fitted by using a three-exponential model. The major fast component had a lifetime of approximately 60 ps, and appeared as fast emission decay at 520 nm and concurrent emission growth at 620 nm, respectively. This component can be associated with the energy transfer from the singlet excited boron dipyrrin to zinc porphyrin. However, the lifetime determined by this method may not be very accurate as it is approaching the time resolution of the instrument (65 ps, fwhm). The second component with a lifetime of 1.6 ns was only observed at 620 nm corresponding to the fluorescence lifetime of zinc porphyrin. In addition, a very weak longest lived component with a lifetime of 2.8 ns was seen only at 520 nm attributed to BDP.

A better time resolution was achieved by using the up-conversion method for the emission decay measurements. Unfortunately, for this method the only available excitation wavelength was 400 nm, at which both the BDP and ZnP chromophores have appreciable absorption. However, the quenching of the BDP chromophore at 520 nm was clearly seen as presented in Figure 8. The best fit of the data was achieved by using a three-exponential model. The two fast decay components had almost equal relative intensities, 40% and 54%, with lifetimes of 9 and 40 ps, respectively. The third longer-lived component was a minor one with contribution less than 6%. The two fast decay components indicate that two conformers of the BDP−ZnP dyad coexist in solution with somewhat different mutual orientations.

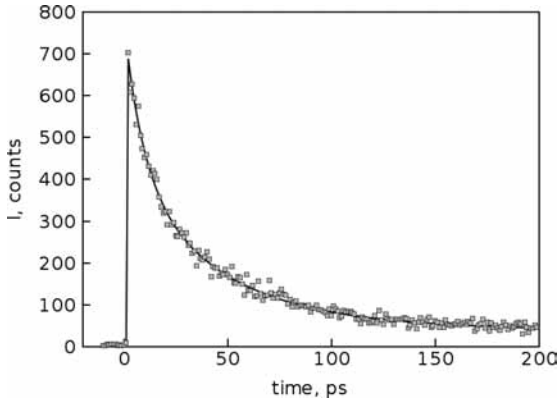

Figure 8. Emission decay of the BDP−ZnP dyad monitored at 520 nm by the up-conversion method in benzonitrile. The solid line presents the data fit (see text). Excitation wavelength was 400 nm.

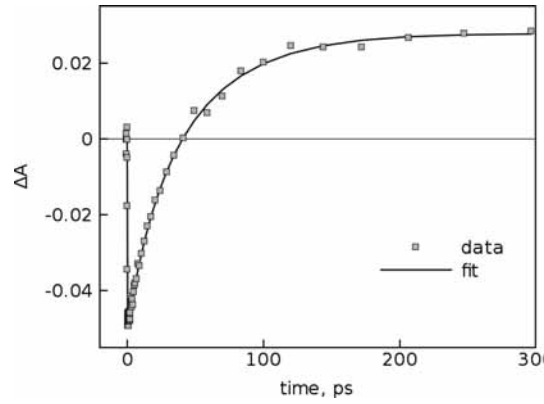

Figure 10. Transient absorption time profile of BDP−ZnP dyad in benzonitrile at 530 nm (squares). The data fit is shown by the solid line. Excitation wavelength was 500 nm.

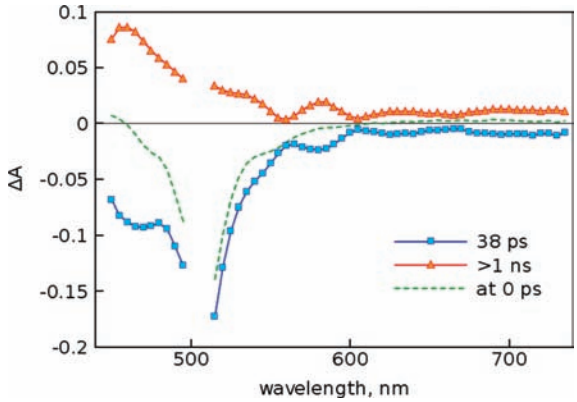

Figure 9. Transient absorption component spectra of BDP−ZnP dyad in benzonitrile (lines with symbols), and time-resolved spectrum right after excitation (dotted line). Excitation wavelength was 500 nm.

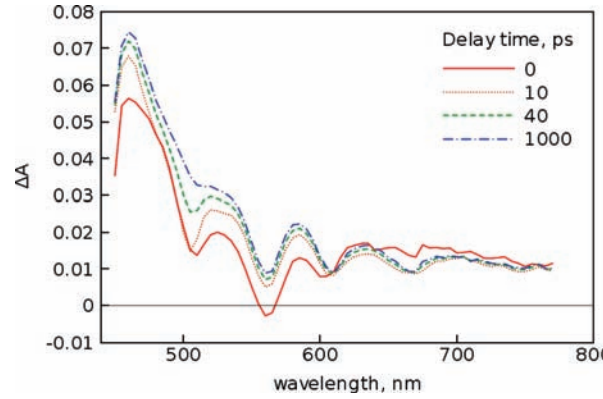

Figure 11. Time resolved transient absorption spectra of BDP−ZnP dyad in benzonitrile. The delay times are indicated in the plot. The excitation wavelength was 410 nm.

The transient absorption measurements with the use of femtosecond pump−probe methods also confirmed the occurrence of efficient energy transfer from BDP to ZnP, as presented in Figure 9. The experiments were carried out with an excitation wavelength of 500 nm to populate the BDP singlet excited state selectively, and analyzed by using a global biexponential fitting of the data. The initial transient absorption spectrum of the dyad (at 0 ps delay time, shown by the dotted line in Figure 9) had characteristic features of the bleached ground state absorption of the BDP chromophore. With a time constant close to 40 ps, the transient absorption spectrum turned into one with characteristic features of the porphyrin singlet excited state (the longest lived component in Figure 9). The transition time correlates well with the emission decay lifetime at 520 nm.

By applying a three-exponential fit to the transient absorption measurements the fit quality was slightly improved and the calculated lifetimes, 18 and 52 ps, matched well with those obtained from up-conversion measurements. An example of fit is presented in Figure 10 for the transient absorption measured at 530 nm. At this wavelength the relative intensities of the fast component were 26% and 74%, respectively.

The absorption maximum of ZnP is located at 431 nm, which could be used for selective excitation of the porphyrin chromophore. Unfortunately this wavelength was not available for excitation for the pump−probe instrument used. The closest available wavelength was 410 nm, at which some fraction of BDP chromophore was also excited. The time-resolved transient absorption spectra obtained with the 410 nm excitation for the BDP−ZnP dyad are presented in Figure 11. The spectrum at zero delay time (right after excitation) revealed characteristic features of both BDP and ZnP singlet excited states. A dip in the absorbance at 500 nm due to the bleaching of the BDP chromophore ground state was observed indicating that some fraction of the chromophore is in the excited state. The appearance of the 460 nm peak and the bleaching at 560 and 600 nm are typical features of the porphyrin singlet excited state. As the delay time increased, the dip at 500 nm disappeared and the absorption at 460 nm increased indicating the energy transfer from BDP to ZnP chromophore.

Upon addition of C_{60} to the solution to form the supramolecular triad, the shapes of the spectra recorded after a few picoseconds and longer delay times changed significantly, as presented in Figure 12. The noteworthy difference is rather strong absorption at the red part of the spectrum (670−750 nm), which is characteristic for the porphyrin cation radical.[29] At the same time in the near-infrared part of the spectrum, the absorption features were broad and rather featureless at the beginning, but at longer delays a band at 1020 nm was noticed (the spectrum at 800 ps in Figure 11), which is indicative of the fullerene anion radical formation. This type of behavior can be explained by a fast formation of the porphyrin−fullerene exciplex, which then relaxes to the charge-separated state, $ZnP^{+\bullet}-C_{60}^{-\bullet}$.[34] The formation of an exciplex is conceivable due to close positioning of zinc porphyrin and fullerene entities in the supramolecular triad as shown in Figure 5a,b.

To gather quantitative information on excited state electron transfer, a global fitting of the transient absorption data was employed. A four-exponential model gave a reasonably small

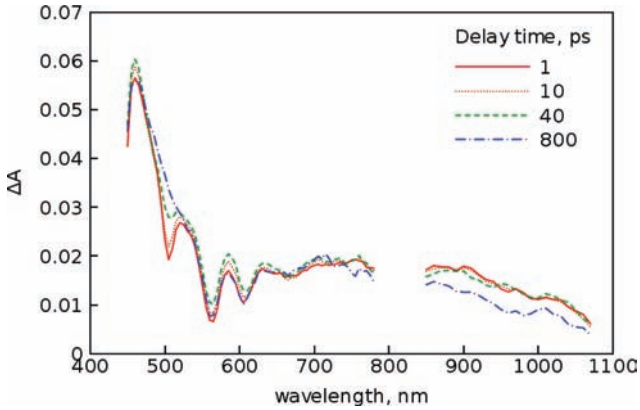

Figure 12. Time resolved transient absorption spectra of BDP−ZnP dyad upon addition of C_{60} (0.6 mM) in benzonitrile. The delay times are indicated in the plot. The excitation wavelength was 410 nm.

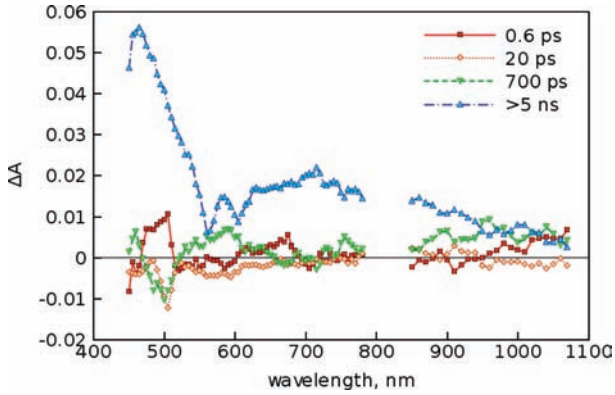

Figure 13. Transient absorption decay component spectra of BDP−ZnP dyad in the presence of C_{60} (0.6 mM) in benzonitrile. The component lifetimes are indicated in the plot. The excitation wavelength was 410 nm.

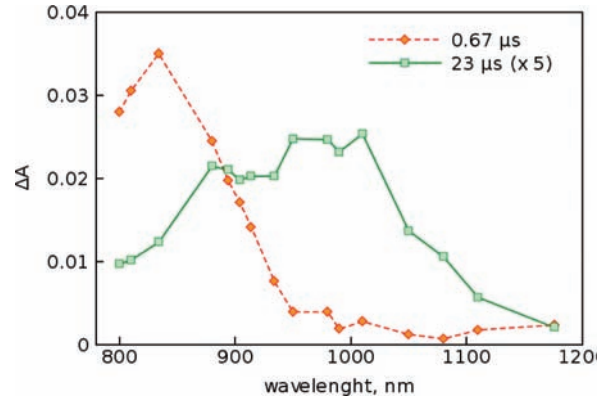

Figure 14. Transient absorption component spectra of BDP−ZnP dyad in the presence of C_{60} (0.6 mM) in benzonitrile obtained by nanosecond laser flash photolysis.

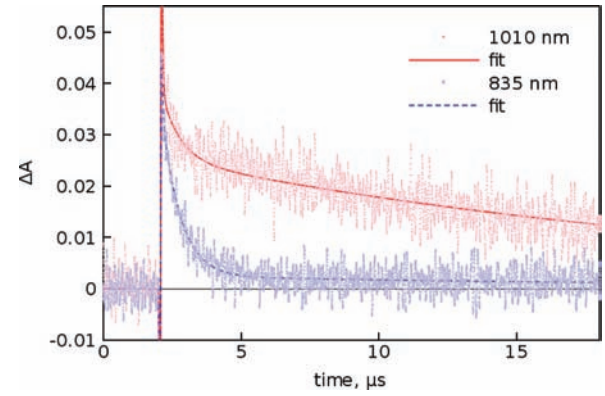

Figure 15. Time profiles of the transient absorption bands of the BDP−ZnP−C_{60} triad (0.6 mM) in benzonitrile at two selected wavelengths.

mean square deviation value ($\sigma = 0.001$), and it was possible to extract three lifetimes in the time scale of the measurements, 0.6, 20, and 700 ps, and a long lifetime extended to nanosecond time domain. The spectra of the decay components are presented in Figure 13. The fast component, 0.6 ps, is most probably due to the internal conversion of the second singlet excited state of ZnP to the first singlet excited state. The second component, 20 ps, showed recovery of the BDP ground state (negative peak at 500 nm), but at the same time it had relatively strong negative intensity in the red part of the spectrum and around 1000 nm, which are characteristic for the formation of the charge-separated state. It seems that two reactions are taking place in the same time domain, that is, the energy transfer from BDP to ZnP and the electron transfer from ZnP to C_{60}. The former is associated with relatively big spectral changes, as can be seen from Figure 9, and the latter has a rather moderate effect on the transient spectra. Although the relative contribution of the excited BDP chromophores was smaller than that of ZnP, the electron transfer time constant from the directly excited ZnP to fullerene was difficult to accurately determine since it interfered strongly with the energy transfer time constant. However, the calculated time constant, 20 ps, was shorter than that for "pure" energy transfer in the BDP−ZnP dyad indicating that porphyrin−fullerene charge separation was somewhat faster than the energy transfer. The latter makes the determination of the charge separation time constant even more difficult when the BDP chromophore was excited (at 500 nm), since in the sequential series of reactions, BDP*−ZnP−C_{60} → BDP−ZnP*−C_{60} → BDP−ZnP^{+}−$C_{60}^{-\bullet}$, population of the BDP−ZnP*−C_{60} intermediate state is never high, i.e., this state is practically unobservable. Hence the transient spectra at a time delay of a few hundred picoseconds had virtually the same shapes at excitation wavelengths of both 410 and 500 nm.

The spectrum of the longest lived component in Figure 13 corresponds to the charge-separated state, BDP−$ZnP^{+\bullet}$−$C_{60}^{-\bullet}$. The lifetime of this state is much longer than the maximum delay time of the pump−probe instrument used (~1 ns). To gather additional information on the CS state lifetime, nanosecond flash photolysis was performed. Since the sample was prepared in an excess of fullerene, two states can be observed in the microsecond time domain: the triplet excited state of fullerene and the CS state. To distinguish between them the transient absorption decays were measured for a number of wavelengths and fitted globally. The results of the fit are presented in Figure 14. The component with lifetime 0.67 μs was attributed to the fullerene triplet state (notice that the measurements were carried out with air saturated solution, and the reference measurements of a pure fullerene sample had virtually the same lifetime as the fullerene triplet state), and the component with the 23 μs lifetime was attributed to the CS state. The decay traces at two characteristic wavelengths are presented in Figure 15. The lifetime of the CS state for the present triad is comparable to the supramolecular triad involving covalently linked ferrocene−zinc porphyrin−crown ether binding to the alkyl ammonium functionalized cation supramolecular triad (lifetime of CS state was 6.2 μs)[35] suggesting charge stabilization to some extent.

Energy Level Diagram. The results of the present investigation along with all of the control experiments clearly show the

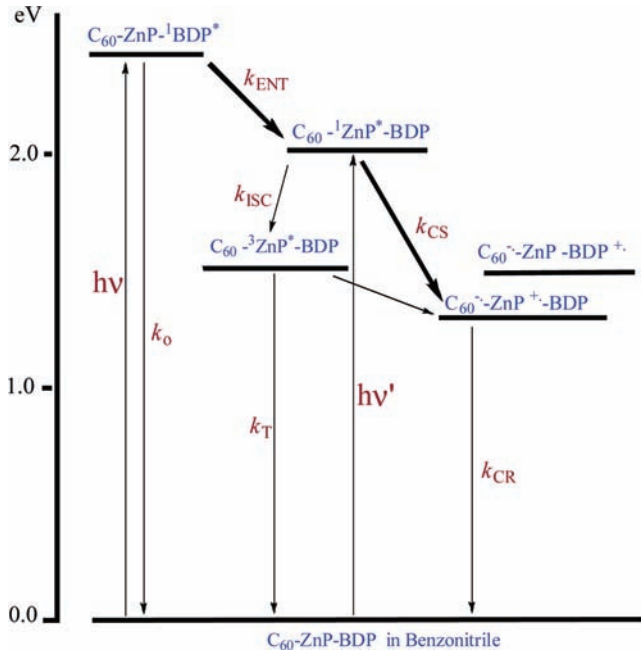

Figure 16. Energy level diagram showing the different photochemical events of the supramolecular C_{60}−ZnP−BDP triad after excitation of either the BDP or ZnP moieties. The thick arrows indicate the major photochemical process and the thin arrows represent the minor photochemical process.

occurrence of efficient energy transfer followed by electron transfer in the studied supramolecular triad. The combination of optical absorption, steady-state fluorescence emission, molecular modeling, electrochemistry, and time-resolved emission and transient absorption studies has permitted the extraction of the needed energetic and kinetic information. The different photochemical events observed in the triad are depicted in Figure 16 in the energy level diagram. Energies of the excited states of the different entities were calculated from the fluorescence peaks while the triplet state energy of ZnP was cited from the literature.[36] The driving forces for the occurrence of electron transfer from the different excited chromophores of the triad used were as discussed earlier. It is also important to note that the difference in free energy change of charge separation for the "close" and "extended" forms of the triad is considered to be negligible. In the energy level diagram, the thick arrows indicate the major processes and the thin arrows are minor processes. On the basis of distance and energetic considerations, an electron transfer from singlet excited BDP to C_{60} is considered to be an inefficient process.

Conclusions

A novel supramolecular triad to mimic the "antenna−reaction center" functionality of the photosynthetic reaction center has been successfully constructed. The antenna mimic, a boron dipyrrin entity, was covalently linked to the reaction center electron donor mimic, a zinc porphyrin possessing a 18-crown-6 entity, as the opposite side of the macrocycle. Both steady-state and time-resolved emission as well as transient absorption studies decidedly proved the occurrence of efficient singlet−singlet energy transfer from BDP to zinc porphyrin with the time scale of 10−50 ps. Next, the reaction center electron acceptor mimic, a fulleropyrrolidine appended with an alkyl ammonium chain, was self-assembled via crown-ether-alkyl ammonium binding to form the supramolecular triad. The structural integrity of the supramolecular triad was derived by optical, computational, and electrochemical studies. Computational studies revealed two possible structures as extreme cases of the supramolecular triad. Energy calculations revealed the possibility of photoinduced electron transfer from singlet excited zinc porphyrin to fullerene. Further time-resolved emission and transient absorption studies demonstrated the occurrence of sequential energy transfer from ^{1}BDP* to ZnP followed by electron transfer from ^{1}ZnP* to fullerene in the supramolecular triad. Nanosecond transient absorption studies revealed the existence of long-lived charge-separated species of $ZnP^{+\bullet}-C_{60}^{-\bullet}$, suggesting that the BDP is also involved in the charge stabilization process due to its facile oxidation.

Experimental Section

Chemicals. Buckminsterfullerene, C_{60} (+99.95%), was from SES Research (Houston, TX). Benzonitrile in a sure seal bottle, sarcosine, 2,4-dimethylpyrrole, trifluoroacetic acid (TFA), dichlorodicyanobenzoquinone (DDQ), and aldehydes were from Aldrich Chemicals (Milwaukee, WI). Tetra-*n*-butylammonium perchlorate, (TBA)ClO_4, was from Fluka Chemicals. All the chromatographic materials and solvents were procured from Fisher Scientific and were used as received. Syntheses and purification of alkyl ammonium functionalized fulleropyrrolidine, zinc porphyrin, and boron dipyrrin used in control experiments were carried out according to the literature procedures.[23]

Synthesis of Boron Dipyrrin−Zinc Porphyrin−Crown Ether Dyad. ***5-(4-Methoxycarbonylphenyl)dipyrromethane (1).*** This compound was prepared according to the general procedure outlined for the synthesis of dipyrromethanes by Lindsey et al.[24] To a pyrrole (68 mL, 0.98 mol) was added methyl 4-formyl benzoate (4 g, 0.024 mol) and the solution was purged with argon for 15 min. Then trifluoroacetic acid (190 μL, 0.0024 mmol) was added and the mixture was stirred at room temperature for 15 min. The mixture was then diluted with CH_2Cl_2 and NaOH (100 mL, 0.1 M) was added, then the organic layer was extracted over Na_2SO_4. The compound was purified by flash column chromatography on silica gel with hexanes: ethyl acetate (60:40 v/v) as eluent. Evaporation of the solvent yielded a pale-yellow solid. Yield 2 g (30%). ^{1}H NMR ($CDCl_3$) δ (ppm) 8.05−7.90 (m, 4H, pyrrole *NH* and phenyl *H*), 7.28 (d, 2H, phenyl *H*), 6.75−6.65 (m, 2H, pyrrole *H*), 6.18−6.12 (m, 2H, pyrrole *H*), 5.92−5.87 (m, 2H, pyrrole *H*), 5.54 (s, 1H, −CH−), 3.90 (s, 3H, $-COOCH_3$).

H_2-5,15-Di(p-methoxycarbonylphenyl)-10,20-di(p-tolyl)porphyrin (2). This compound was prepared according to Luo et al.[25] A solution of **1** (1.6 g, 5.71 mmol) was added to *p*-tolylaldehyde (675 μL, 5.71 mmol) in $CHCl_3$, and the reaction mixture was stirred under argon for 1 h. Then $BF_3 \cdot O(Et)_2$ (724 μL, 5.71 mmol) was added, and the reaction mixture was stirred in the dark for 2 h. *p*-Chloranil (2.11 g, 8.57 mmol) was added to the reddish-black reaction mixture, and the resulting mixture was stirred for 18 h. Triethylamine (2.4 mL, 17.25 mmol) was added, and the reaction mixture was stirred for 1 h and then concentrated. Column chromatography on silica gel with chloroform as eluent gave a mixture of five porphyrins including the titled compound. Subsequent column chromatography of this fraction on silica gel with toluene:$CHCl_3$ (70:30 v/v) as eluent yielded the titled compound as the third band. Evaporation of the solvent yielded the desired compound as a purple solid. Yield 208 mg (5%). ^{1}H NMR ($CDCl_3$) δ (ppm) 8.82 (dd, 8H, β-pyrrole *H*), 8.42 (d, 4H, phenyl *H*), 8.25 (d, 4H, phenyl *H*), 8.10 (d, 4H, phenyl *H*), 7.58 (d, 4H, phenyl *H*), 4.12 (s, 6H, $-COOCH_3$),

2.7 (s, 6H, $-CH_3$), −2.80 (s, br, 2H, −NH). ESI mass (in $CHCl_3$) calcd 758.8, found [M + 1] 759.9.

H_2-5,15-Di(p-carboxyphenyl)-10,20-di(p-tolyl)porphyrin (3).[25] A suspension of **2** (200 mg, 0.264 mmol) in THF:ethanol (1:1) was taken in a 250 mL round-bottomed flask and potassium hydroxide (1.5 g, 0.027 mol) dissolved in water (12 mL) was added to it. The reaction mixture was refluxed for 8 h. After cooling, the solvent was evaporated; the residue was diluted with water (100 mL) and then filtered. The desired compound was obtained as the dipotassium salt. The aqueous suspension of porphyrin dipotassium salt was acidified with concentrated HCl (pH 2) and then filtered. The title compound was obtained as a purple powder and used without further purification. Yield 85 mg (44%). ^{1}H NMR (DMSO-*d*) δ (ppm) 8.8 (dd, 8H, β-pyrrole *H*), 8.38 (d, 8H, phenyl *H*), 8.18−8.10 (d, 4H, phenyl *H*), 7.65−7.55 (d, 4H, phenyl *H*), 2.55 (s, 6H, $-CH_3$), −2.40−2.95 (s, br, 2H, −NH).

1-(Difluoroboryl)-2-[(Z)-(3,5-dimethyl-2H-pyrrol-2-ylidene)(4-nitrophenyl)methyl]-3,5-dimethyl-1H-pyrrole (4).[19d] 2,4-Dimethylpyrrole (1.08 mL, 10.5 mmol) and 4-nitrobenzaldehyde (0.93 g, 6.2 mmol) were added to CH_2Cl_2 (600 mL) and purged with N_2, then trifluoroacetic acid (0.09 mL, 1.23 mmol) was added and the mixture was stirred for 2 h. The resulting solution was washed with 0.1 M NaOH (200 mL) and then water, dried over anhydrous Na_2SO_4, and filtered, then the solvent was evaporated. Next the product was redissolved in methylene chloride, and *p*-chloranil (1.36 g, 5.5 mmol) was added to the mixture. The resulting mixture was stirred for 10 min, then triethylamine (4 mL) and born trifluoride etherate (3.5 mL) were added to the mixture. After 1 h of stirring, the resulting solution was poured into water and the compound was extracted with methylene chloride. The compound was purified by flash column chromatography on silica gel with hexanes:$CHCl_3$ (60:40 v/v) as eluent. Evaporation of the solvent yielded 900 mg of the desired product. ^{1}H NMR ($CDCl_3$) δ (ppm) 8.39 (d, 2H, phenyl *H*), 7.55 (d, 2H, phenyl *H*), 6.02 (s, 2H, pyrrole *H*), 2.55 (s, 6H, $-CH_3$), 1.37 (s, 6H, $-CH_3$). ESI mass (in CH_2Cl_2) calcd 369.2, found [M + 1] 370.5.

1-(Difluoroboryl)-2-[(Z)-(3,5-dimethyl-2H-pyrrol-2-ylidene)(4-aminophenyl)methyl]-3,5-dimethyl-1H-pyrrole (5). A solution of **4** (100 mg) in THF (40 mL) was hydrogenated over 5% Pd on charcoal (300 mg) at room temperature and atmospheric pressure. Then, the catalyst was removed by filtration with use of Celite, and the filtrate was evaporated. The compound was purified by flash column chromatography on silica gel with toluene as eluent. Evaporation of the solvent yielded 36 mg of **5**, 40%. ^{1}H NMR($CDCl_3$) δ (ppm) 7.00 (d, 2H, phenyl *H*), 6.78 (d, 2H, phenyl *H*), 5.96 (s, 2H, pyrrole *H*), 3.47 (br s, 2H, $-NH_2$), 2.55 (s, 6H, $-CH_3$), 1.49 (s, 6H, $-CH_3$). ESI mass (in CH_2Cl_2) calcd 339.2, found [M + 1] 340.3.

H_2-5-{4-[2-(4-Benzo-[18-crown-6])amido]phenyl}-15-{4-[2-(4-difluoroboron dipyrrinylphenyl)amido]phenyl}-10,20-di(p-tolyl)porphyrin (6). Compound **3** (40 mg, 0.05 mmol) was taken in dry toluene (20 mL) then thionyl chloride (80 μL, 1.1 mmol) and pyridine (80 μL) were added and the reaction mixture was refluxed under argon for 3 h. After cooling, the solvent was evaporated and the resulting green compound was redissolved in dry toluene (25 mL). Then, pyridine (210 μL) was added followed by **5** (18 mg, 0.05 mmol) and 4′-amino benzo-[18-crown-6] (18 mg, 0.05 mmol). The reaction mixture was allowed to stir at room temperature under argon for 12 h. The solvent was evaporated and the crude compound was purified by column chromatography on silica gel with hexanes:$CHCl_3$ (10:90 v/v). Evaporation of the solvent yielded the desired compound (24 mg). ^{1}H NMR (CDCl3) δ (ppm) 8.95−8.75 (m, 8H, β-pyrrole *H*), 8.40−8.18 (m, 8H, phenyl *H*), 8.10 (d, 4H, phenyl *H*), 7.85 (d, 2H, BDP phenyl *H*), 7.56 (d, 4H, phenyl *H*), 7.35−7.28 (m, 1H, benzo-crown phenyl *H*), 7.12−7.05 (m, 1H, benzo-crown phenyl *H*), 6.90 (d, 1H, benzo-crown phenyl *H*), 6.02 (s, 2H, pyrrole *H*), 4.30−4.18 (m, 4H, crownethylene *H*), 4.00−3.90 (m, 4H, crownethylene *H*), 3.82−3.70 (m, 12H, crownethylene *H*), 2.70 (s, 6H, phenyl CH_3), 2.60 (s, 6H, pyrrole CH_3), 1.65 (s, 6H, pyrrole CH_3), −2.78 (s, br, 2H, −NH). ESI mass (in $CHCl_3$) calcd 1400.3 (with K^+), found [M + 1] (with K^+) 1401.2.

H_2-5-{4-[2-(4-Benzo-[18-crown-6])amido]phenyl}-15-{4-[2-(4-difluoroboron dipyrrinylphenyl)amido]phenyl}-10,20-di(p-tolyl)porphyrinato Zinc(II) (7). The free-base porphyrin **6** (20 mg) was dissolved in $CHCl_3$ (10 mL) then a saturated solution of zinc acetate in methanol was added to the solution, and the resulting mixture was refluxed for 2 h until the 515 nm band of free-base porphyrin had disappeared.[36] At the end, the reaction mixture was washed with water and dried over anhydrous Na_2SO_4. Chromatography on silica gel column by using hexanes: $CHCl_3$ (10:90 v/v) gave the title compound. Yield 20 mg (90%). ^{1}H NMR ($CDCl_3$) δ (ppm) 9.00−8.80 (m, 8H, β-pyrrole *H*), 8.43−8.21 (m, 8H, phenyl *H*), 8.12 (d, 4H, phenyl *H*), 7.88 (d, 2H, BDP phenyl *H*), 7.58 (d, 4H, phenyl *H*), 7.35−7.28 (m, 1H, benzo-crown phenyl *H*), 7.07−7.00 (m, 1H, benzo-crown phenyl *H*), 6.85 (d, 1H, benzo-crown phenyl *H*), 6.01 (s, 2H, pyrrole *H*), 4.28−4.15 (m, 4H, crownethylene *H*), 4.38−3.87 (m, 4H, crownethylene *H*), 3.79−3.76 (m, 12H, crownethylene *H*), 2.70 (s, 6H, phenyl CH_3), 2.62 (s, 6H, pyrrole CH_3), 1.69 (s, 6H, pyrrole CH_3). ESI mass (in $CHCl_3$) calcd 1463.7 (with K^+), found [M + 1] (with K^+) 1464.6.

Instrumentation. The UV−visible spectral measurements were carried out with a Shimadzu Model 1600 UV−visible spectrophotometer. The fluorescence emission was monitored by using a Varian Eclipse spectrometer. A right angle detection method was used. The ^{1}H NMR studies were carried out on a Varian 400 MHz spectrometer. Tetramethylsilane (TMS) was used as an internal standard. Cyclic voltammograms were recorded on a EG&G PARSTAT electrochemical analyzer, using a three-electrode system. A platinum button electrode was used as the working electrode. A platinum wire served as the counter electrode and a Ag/AgCl electrode was used as the reference electrode. Ferrocene/ferrocenium redox couple was used as an internal standard. All the solutions were purged prior to electrochemical and spectral measurements with argon gas. The computational calculations were performed by ab initio B3LYP/3-21G(*) methods with the Gaussian 98[29] software package on high-speed PCs. The ESI-mass spectral analyses of the newly synthesized compounds were performed by using a Fennigan LCQ-Deca mass spectrometer. For this, the compounds (about 0.1 mM concentration) were prepared in CH_2Cl_2, freshly distilled over calcium hydride.

Time-Resolved Fluorescence and Transient Absorption Measurements.[37] Fluorescence decays of the samples in the nanosecond and subnanosecond time scales were measured by using a time-correlated single photon counting (TCSPC) system (PicoQuant GmBH) consisting of PicoHarp 300 controller and PDL 800-B driver. The samples were excited with the pulsed diode laser head LDH-P-C-485 at 485 nm and fluorescence decays were measured at the wavelengths of emission maxima. The signals were detected with a microchannel plate photomultiplier tube (Hamamatsu R2809U). The time resolution of the TCSPC measurements was about 60−70 ps (fwhm of the instrument response function).

An up-conversion instrument (FOG-100, CDP Corp.) for time-resolved fluorescence was used to detect the fast processes with a time resolution of ~200 fs. The primary Ti:sapphire generator (TiF-50, CDP Corp.) was pumped by Nd CW laser (Verdi-6, Coherent Inc.), and a second harmonic (~410 nm) was used to excite the sample solution in a rotating cuvette. Emission from the sample was collected to a nonlinear crystal (NLC), where it was mixed with the so-called gate pulse, which was the laser fundamental. The signal was measured at a sum frequency of the gate pulse and the selected emission maximum of the sample. The gate pulses were passed through a delay line so that it arrived at NLC at a desired time after sample excitation. By scanning through the delay line the emission decay curve of the sample was detected.

Pump−probe and up-conversion techniques for time-resolved absorption and fluorescence, respectively, were used to detect the fast processes with a time resolution shorter than 0.2 ps. The instrument and the data analysis procedure used have been described earlier.[37]

Acknowledgment. The authors are thankful to National Science Foundation (Grant 0804015 to FD) and the Academy of Finland for support of this work.

References and Notes

(1) (a) Barber, J.; Anderson, B. *Nature* **1994**, *370*, 31. (b) Fromme, P. *Curr. Opin. Struct. Biol.* **1996**, *6*, 473. (c) Krauss, N.; Schubert, W. D.; Klukas, O.; Fromme, P.; Witt, H. T.; Saenger, W. *Nat. Struct. Biol.* **1996**, *3*, 965. (d) *The Photosynthetic Reaction Center*; Deisenhofer, J., Norris, J. R., Eds.; Academic Press: San Diego, CA, 1993. (e) Deisenhofer, J.; Epp, O.; Miki, K.; Huber, R.; Michel, H. *J. Mol. Biol.* **1984**, *180*, 385.

(2) (a) *Introduction of Molecular Electronics*, Petty, M. C., Bryce, M. R., Bloor, D., Eds.; Oxford University Press: New York, 1995. (b) *Molecular Electronics: Science and Technology*; Aviram, A., Ratner, M., Eds.; New York Academy of Science: New York, 1998; p 852. (c) *Molecular Switches*, Feringa, B. L., Ed.; Wiley-VCH GmbH: Weinheim, Germany, 2001. (d) Gust, D.; Moore, T. A.; Moore, A. L. *Chem. Commun.* **2006**, 1169–1178. (e) Balzani, V.; Credi, A.; Venturi, M. In *Organic Nanostructures*; ed. Atwood, J. L., Steed, J. W., Eds.; Wiley-VCH: Weinheim, Germany, 2008; pp 1−31.

(3) (a) Connolly, J. S., Ed. *Photochemical Conversion and Storage of Solar Energy*; Academic:, New York, 1981. (b) Wasielewski, M. R. *Chem. Rev.* **1992**, *92*, 435. (c) Verhoeven, J. W. *Adv. Chem. Phys.* **1999**, *106*, 603. (d) Osuka, A.; Mataga, N.; Okada, T. *Pure Appl. Chem.* **1997**, *69*, 797. (e) Flamigni, L.; Barigelletti, F.; Armaroli, N.; Collin, J.-P.; Dixon, I. M.; Sauvage, J.-P.; Williams, J. A. G. *Coord. Chem. Rev.* **1999**, *190−192*, 671. (f) Diederich, F.; Gomez-Lopez, M. *Chem. Rev. Soc.* **1999**, *28*, 263.

(4) (a) Blanco, M.-J.; Consuelo Jimenez, M.; Chambron, J.-C.; Heitz, V.; Linke, M.; Sauvage, J.-P. *Chem. Rev. Soc.* **1999**, *28*, 293. (b) Balzani, V.; Ceroni, P.; Juris, A.; Venturi, M.; Campagna, S.; Puntoriero, F.; Serroni, S. *Coord. Chem. Rev.* **2001**, *219*, 545. (c) Balzani, V.; Credi, A.; Venturi, M. *ChemSusChem* **2008**, *1*, 26.

(5) (a) Bixon, M.; Fajer, J.; Feher, G.; Freed, J. H.; Gamliel, D.; Hoff, A. J.; Levanon, H.; Möbius, K.; Nechushtai, R.; Norris, J. R.; Scherz, A.; Sessler, J. L.; Stehlik, D. *Isr. J. Chem.* **1992**, *32*, 449. (b) Lewis, F. D.; Letsinger, R. L.; Wasielewski, M. R. *Acc. Chem. Res.* **2001**, *34*, 159.

(6) (a) Gust, D.; Moore, T. A.; Moore, A. L. *Acc. Chem. Res.* **1993**, *26*, 198. (b) Gust, D.; , Moore, T. A. In *The Porphyrin Handbook*, Kadish, K. M., Smith, K., Guilard, R., Eds.; Academic Press: San Diego, 2000; Vol. 8, pp 153−190.

(7) (a) Fukuzumi, S.; Guldi, D. M. In *Electron Transfer in Chemistry*; Balzani, V., Ed.; Wiley-VCH: Weinheim, Germany, 2001; Vol. 2, pp 270−337. (b) Fukuzumi, S. In *The Porphyrin Handbook*; Kadish, K. M., Smith, K., Guilard, R., Eds.; Academic Press: San Diego, CA, 2000; Vol. 8, pp 115−151. (c) Fukuzumi, S. *Phys. Chem. Chem. Phys.* **2008**, *10*, 2283. (d) Imahori, H.; Sekiguchi, Y.; Yukiyasu, S.; Tohru, A.; Araki, Y.; Ito, O.; Yamada, H.; Fukuzumi, S. *Chem.−Eur. J.* **2004**, *10*, 3184. (e) Fukuzumi, S.; Kotani, H.; Ohkubo, K.; Ogo, S.; Tkachenko, J. V.; Lemmetyinen, H. *J. Am. Chem. Soc.* **2004**, *126*, 1600.

(8) (a) Sakata, Y.; Imahori, H.; Tsue, H.; Higashida, S.; Akiyama, T.; Yoshizawa, E.; Aoki, M.; Yamada, K.; Hagiwara, K.; Taniguchi, S.; Okada, T. *Pure Appl. Chem.* **1997**, *69*, 1951. (b) Imahori, H.; Sakata, Y. *Eur. J. Org. Chem.* **1999**, 2445. (c) Imahori, H.; Tamaki, K.; Araki, Y.; Sekiguchi, Y.; Ito, O.; Sakata, Y.; Fukuzumi, S. *J. Am. Chem. Soc.* **2002**, *124*, 5165. (d) Umeyama, T.; Imahori, H. *Energy Environ. Sci.* **2008**, *1*, 120.

(9) (a) Guldi, D. M. *Chem. Commun.* **2000**, 321. (b) Guldi, D. M. *Chem. Soc. Rev.* **2002**, *31*, 22. (c) Sgobba, V.; Guldi, D. M. *Chem. Soc. Rev.* **2009**, *38*, 165. (d) Mateo-Alonso, A.; Guldi, D. M.; Paolucci, F.; Prato, M. *Angew. Chem., Int. Ed.* **2007**, *46*, 8120. (e) Guldi, D. M. *Phys. Chem. Chem. Phys.* **2007**, *9*, 1400. (f) Sanchez, L.; Nazario, M.; Guldi, D. M. *Angew. Chem., Int. Ed.* **2005**, *44*, 5374.

(10) Sessler, J. S.; Wang, B.; Springs, S. L.; Brown, C. T. In *Comprehensive Supramolecular Chemistry*; Atwood, J. L., Davies, J. E. D., MacNicol, D. D., Vögtle, F., Eds.; Pergamon: New York, 1996; Chapter 9.

(11) (a) El-Khouly, M. E.; Ito, O.; Smith, P. M.; D'Souza, F. *Photochem. Photobiol. C* **2004**, *5*, 79. (b) D'Souza, F.; Ito, O. *Coord. Chem. Rev.* **2005**, *249*, 1410. (c) D'Souza, F.; Ito, O. In *Handbook of Organic Electronics and Photonics*; Nalwa, H. R., Ed.; American Scientific Publishers: Stevenson Ranch, CA, 2008; Vol. 1, Chapter 13, pp 485−521. (d) Chitta, R.; D'Souza, F. *J. Mater. Chem.* **2008**, *18*, 1440.

(12) (a) Seth, J.; Palaniappna, V.; Wagner, R. W.; Johnson, T. E.; Lindsey, J. S.; Holten, D.; Bocian, D. F. *J. Am. Chem. Soc.* **1996**, *118*, 11194. (b) Hsiao, J.-S.; Krueger, B. J.; Wagner, R. W.; Johnson, T. E.; Delaney, J. K.; Mauzerall, D. C.; Fleming, G. R.; Lindsey, J. S.; Bocian, D. F.; Donohoe, R. J. *J. Am. Chem. Soc.* **1996**, *118*, 11181. (c) Seth, J.; Palaniappan, V.; Johnson, T. E.; Prathapan, S.; Lindsey, J. S.; Bocian, D. F. *J. Am. Chem. Soc.* **1994**, *116*, 10578.

(13) (a) Sessler, J. L.; Magda, D. J.; Harriman, A. *J. Am. Chem. Soc.* **1995**, *117*, 704. (b) Kral, V.; Springs, S. L.; Sessler, J. L. *J. Am. Chem. Soc.* **1995**, *11*, 7–8881. (c) Springs, S. L.; Gosztola, D.; Wasielewski, M. R.; Kral, V.; Andrievsky, A.; Sessler, J. L. *J. Am. Chem. Soc.* **1999**, *121*, 2281. (d) Bothner-By, A. A.; Dodok, J.; Johnson, T. E.; Delaney, J. K.; Lindsey, J. S. *J. Phys. Chem.* **1996**, *100*, 17551.

(14) Luo, C.; Guldi, D. M.; Imahori, H.; Tamaki, K.; Sakata, Y. *J. Am. Chem. Soc.* **2000**, *122*, 6535.

(15) (a) Wagner, R. W.; Johnson, T. E.; Lindsey, J. S. *J. Am. Chem. Soc.* **1996**, *118*, 11166. (b) Strachan, J. P.; Gentemann, S.; Seth, J.; Kalsback, W. A.; Lindsey, J. S.; Holten, D.; Bocian, D. F. *J. Am. Chem. Soc.* **1997**, *119*, 11191. (c) Li, F.; Gentemann, S.; Kalsbeck, W. A.; Seth, J.; Lindsey, J. S.; Holten, D.; Bocian, D. F. *J. Mater. Chem.* **1997**, *7*, 1245.

(16) (a) Giribabu, L.; Kumar, A.; Neeraja, V.; Maiya, B. G. *Angew. Chem., Int. Ed.* **2001**, *40*, 3621. (b) Aratani, N.; Cho, H. S.; Ahn, T. K.; Cho, S.; Kim, D.; Sumi, H.; Osuka, A. *J. Am. Chem. Soc.* **2003**, *125*, 9668. (c) Shinmori, H.; Ahn, T. K.; Cho, H. S.; Kim, D.; Yoshida, N.; Osuka, A. *Angew. Chem., Int. Ed.* **2003**, *42*, 2754. (d) Choi, M.-S.; Aida, T.; Yamazaki, T.; Yamazaki, I. *Chem.−Eur. J.* **2002**, *8*, 2667. (e) Choi, M.-S.; Aida, T.; Luo, H.; Araki, Y.; Ito, O. *Angew. Chem., Int. Ed.* **2003**, *42*, 4060.

(17) (a) Splan, K. E.; Keefe, M. H.; Massari, A. M.; Walters, K. A.; Hupp, J. T. *Inorg. Chem.* **2002**, *41*, 619. (b) Nakano, A.; Yasuda, Y.; Yamazaki, T.; Akimoto, S.; Yamazaki, I.; Miyasaka, H.; Itaya, A.; Murakami, M.; Osuka, A. *J. Phys. Chem. A* **2001**, *105*, 4822.

(18) (a) Wagner, R. W.; Lindsey, J. S. *J. Am. Chem. Soc.* **1994**, *116*, 9759. (b) Wagner, R. W.; Lindsey, J. S.; Seth, J.; Palaniappna, V.; Bocian, D. F. *J. Am. Chem. Soc.* **1996**, *118*, 3996. (c) Abbroise, A.; Wagner, R. W.; Rao, P. D.; Riggs, J. A.; Hascoat, P.; Diers, J. R.; Seth, L.; Robin, K.; Bocian, D. F.; Holten, D.; Lindsey, J. S. *Chem. Mater.* **2001**, *13*, 1023. (d) Ambroise, A.; Kirmaier, C.; Wagner, R. W.; Loewe, R. S.; Bocian, D. F.; Holten, D.; Lindsey, J. S. *J. Org. Chem.* **2002**, *67*, 3811.

(19) (a) Kuciauskas, D.; Liddell, P. A.; Lin, S.; Johnson, T. E.; Weghorn, S. J.; Lindsey, J. S.; Moore, A. L.; Moore, T. A.; Gust, D. *J. Am. Chem. Soc.* **1999**, *121*, 8604. (b) Kodis, G.; Liddell, P. A.; de la Garza, L.; Clausen, C.; Lindsey, J. S.; Moore, A. L.; Moore, T. A.; Gust, D. *J. Phys. Chem. A* **2002**, *106*, 2036. (c) Tamaki, K.; Imahori, H.; Nishimura, Y.; Yamazaki, I.; Sakata, Y. *Chem. Commun.* **1999**, 625. (d) Imahori, H.; Norieda, H.; Yamada, H.; Nishimura, Y.; Yamazaki, I.; Sakata, Y.; Fukuzumi, S. *J. Am. Chem. Soc.* **2001**, *123*, 100.

(20) (a) Liddell, P. A.; Kodis, G.; de la Garza, L.; Moore, A. L.; Moore, T. A.; Gust, D. *J. Phys. Chem. B* **2004**, *108*, 10256. (b) Kodis, G.; Terazono, Y.; Liddell, P. A.; Andreasson, J.; Garg, V.; Hambourger, M.; Moore, A. L.; Moore, T. A.; Gust, D. *J. Am. Chem. Soc.* **2006**, *128*, 1818. (c) Terazono, Y.; Kodis, G.; Liddell, P. A.; Garg, V.; Moore, T. A.; Moore, A. L.; Gust, D. *J. Phys. Chem. B* **2009**, *113*, 7147.

(21) (a) D'Souza, F.; Smith, P. M.; Zandler, M. E.; McCarty, A. L.; Itou, M.; Araki, Y.; Ito, O. *J. Am. Chem. Soc.* **2004**, *126*, 7898. (b) Wolffs, M.; Hoeben, F. J. M.; Beckers, E. H. A.; Schenning, A. P. H. J.; Meijer, E. W. *J. Am. Chem. Soc.* **2005**, *127*, 12484. (c) D'Souza, F.; Gadde, S.; Islam, D. J. S.; Wijesinghe, C. A.; Schumacher, A. L.; Zandler, M. E.; Araki, Y.; Ito, O. *J. Phys. Chem. A* **2007**, *111*, 8552. (d) Kuramochi, Y.; Sandanayaka, A. S. D.; Satake, A.; Araki, Y.; Ogawa, K.; Ito, O.; Kobuke, Y. *Chem.−Eur. J.* **2009**, *15*, 2317.

(22) (a) Loudet, A.; Burgess, K. *Chem. Rev.* **2007**, *107*, 4891. (b) Li, F.; Yang, S. I.; Ciringh, T.; Seth, J.; Martin, C. H., III.; Singh, D. L.; Kim, D.; Birge, R. R.; Bocian, D. F.; Holten, D.; Lindsey, J. S. *J. Am. Chem. Soc.* **1998**, *120*, 10001.

(23) (a) D'Souza, F.; Chitta, R.; Gadde, S.; Zandler, M. E.; McCarty, A. L.; Sandanayaka, A. S. D.; Araki, Y.; Ito, O. *Chem.−Eur. J.* **2005**, *11*, 4416. (b) D'Souza, F.; Chitta, R.; Gadde, S.; Zandler, M. E.; Sandanayaka, A. S. D.; Araki, Y.; Ito, O. *Chem. Commun.* **2005**, 1279. (c) Solladie, N.;

Walther, M. E.; Gross, M.; Duarte, M. F.; Bourgogne, C.; Nierengarten, J.-F. *Chem. Commun.* **2003**, 2412. (d) Nierengarten, J.-F.; Hahn, U.; Duarte, M. F.; Cardinali, F.; Solladie, N.; Walther, M. E.; Dorsselaer, A. V.; Herschbach, H.; Leize, E.; Gary, A.; Trabolsi, A.; Elhabiri, M. C. R. *C. R. Chim.* **2006**, *9*, 1022.

(24) Lee, C. H.; Lindsey, J. S. *Tetrahedron* **1994**, *50*, 39–11427.

(25) Luo, C.; Guldi, D. M.; Imahori, H.; Tamaki, K.; Sakata, Y. *J. Am. Chem. Soc.* **2000**, *122*, 6535.

(26) *Principles of Fluorescence Spectroscopy*, 3rd ed.; Lakowicz, J. R.; Springer: New York, 2006.

(27) D'Souza, F.; Chitta, R.; Gadde, S.; Zandler, M. E.; McCarty, A. L.; Sandanayaka, A. S. D.; Araki, Y.; Ito, O. *J. Phys. Chem. A* **2006**, *110*, 4338.

(28) Benesi, H. A.; Hildebrand, J. H. *J. Am. Chem. Soc.* **1949**, *71*, 2703.

(29) Frisch, M. J.; Trucks, G. W.; Schlegel, H. B.; Scuseria, G. E.; Robb, M. A.; Cheeseman, J. R.; Zakrzewski, V. G.; Montgomery, J. A.; Stratmann, R. E.; Burant, J. C.; Dapprich, S.; Millam, J. M.; Daniels, A. D.; Kudin, K. N.; Strain, M. C.; Farkas, O.; Tomasi, J.; Barone, V.; Cossi, M.; Cammi, R.; Mennucci, B.; Pomelli, C.; Adamo, C.; Clifford, S.; Ochterski, J.; Petersson, G. A.; Ayala, P. Y.; Cui, Q.; Morokuma, K.; Malick, D. K.; Rabuck, A. D.; Raghavachari, K.; Foresman, J. B.; Cioslowski, J.; Ortiz, J. V.; Stefanov, B. B.; Liu, G.; Liashenko, A.; Piskorz, P.; Komaromi, I.; Gomperts, R.; Martin, R. L.; Fox, D. J.; Keith, T.; Al-Laham, M. A.; Peng, C. Y.; Nanayakkara, A.; Gonzalez, C.; Challacombe, M.; Gill, P. M. W.; Johnson, B. G.; Chen, W.; Wong, M. W.; Andres, J. L.; Head-Gordon, M.; Replogle, E. S.; Pople, J. A. *Gaussian 98*, Revision A.9, Gaussian, Inc., Pittsburgh, PA, 1998.

(30) For computational applictions of supramolecular porphyrin−fullerene systems see: (a) Zandler, M. E.; D'Souza, F. *C. R. Chim.* **2006**, *9*, 960. (b) Zandler, M. E.; D'Souza, F. In *DFT Calculations on Fullerenes and Carbon Nanotubes*; Basiuk, V. A., Irle, S., Eds.; Research Signpost: Kerala, India, 2008; pp 81−126.

(31) (a) Balch, A. L.; Olmstead, M. M. *Coord. Chem. Rev.* **1999**, *185−186*, 601. (b) Boyd, P. D. W.; Reed, C. A. *Acc. Chem. Res.* **2005**, *38*, 235.

(32) *Electrochemical Methods: Fundamentals and Applications*, 2nd ed; Bard, A. J., Faulkner, L. R., Eds.; John Wiley: New York, 2001.

(33) Weller, A. Z. *Phys. Chem.* **1982**, *132*, 93.

(34) (a) Tkachenko, N. V.; Lemmetyinen, H.; Sonoda, J.; Ohkubo, K.; Sato, T.; Imahori, H.; Fukuzumi, S. *J. Phys. Chem. A* **2003**, *107*, 8834–8844. (b) Kira, A.; Tanaka, M.; Umeyama, T.; Matano, Y.; Yoshimoto, N.; Zhang, Y.; Ye, S.; Lehtivuori, H.; Tkachenko, N. V.; Lemmetyinen, H.; Imahori, H. *J. Phys. Chem. C* **2007**, *111*, 13618.

(35) D'Souza, F.; Chitta, R.; Gadde, S.; Islam, D. M. S.; Schumacher, A. L.; Zandler, M. E.; Araki, Y.; Ito, O. *J. Phys. Chem. B* **2006**, *110*, 25240.

(36) Smith, K. M. *Porphyrins and Metalloporphyrins*; Elsevier: New York, 1977.

(37) (a) Tkachenko, N. V.; Rantala, L.; Tauber, A. Y.; Helaja, J.; Hynninen, P. H.; Lemmetyinen, H. *J. Am. Chem. Soc.* **1999**, *121*, 9378. (b) Vehmanen, V.; Tkachenko, N. V.; Imahori, H.; Fukuzumi, S.; Lemmetyinen, H. *Spectrochim. Acta. A* **2001**, *57*, 2229. (c) Isosomppi, M.; Tkachenko, N. V.; Efimov, A.; Lemmetyinen, H. *J. Phys. Chem. A* **2005**, *109*, 4881–4890.

(38) (a) Kim, K. S.; Tarakeshwar, P.; Lee, J. Y. *Chem. Rev.* **2000**, *100*, 4145. (b) Jensen, K. P.; Ryde, U. *J. Phys. Chem. A* **2003**, *107*, 7539.

JP9032194